A Robust Multi-view Freehand Three-dimensional Ultrasound Imaging System Using Volumetric Registration

Honggang Yu[1], Marios S. Pattichis[1] and M. Beth Goens[2]

[1]image and video Processing and Communications Lab (ivPCL)
Department of Electrical and Computer Engineering
[2]Children's Hospital Heart Center, The University of New Mexico
Albuquerque, NM, USA

Abstract - *In this paper, we describe a freehand, three-dimensional ultrasound imaging system. The system uses an electromagnetic position and orientation measurement device to capture two-dimensional ultrasound images at arbitrary planar orientations in space. For robust performance, we use a novel electromagnetic interference detection algorithm that can be used to estimate the probability density function of position and orientation measurement errors.*

Another important contribution of the proposed system is its ability to reconstruct from multiple standard views. The multi-view reconstruction procedure results in significant reduction in reconstruction error. The system uses object-based 3D volume registration, allowing for arbitrary rigid object movements in inter-view acquisition.

The proposed system has been validated on simulated data and a physical, 3D ultrasound calibration phantom. Quantitative experimental results demonstrate the effectiveness of the 3D registration system, and a significant reduction in the mean-squared error via the use of the proposed multi-view reconstruction method.

Keywords: freehand, 3D ultrasound, 3D reconstruction, interference detection, multiple-view, volume registration.

1. Introduction

Freehand 3D ultrasound imaging techniques can be used to reconstruct 3D objects from a set of registered 2D image slices. The 2D slices can be located at any arbitrary orientation and position throughout space, and can be acquired using any standard, 2D ultrasound transducer in conjunction with an orientation and position sensor. This strategy allows large volumes to be imaged and offers the possibility to upgrade a conventional 2D scanner to a 3D scanner, at a very low cost. Recently, 3D ultrasound imaging systems have been used for diagnosis in clinical echocardiography [1].

Most research on 3D freehand ultrasound has focused on a single reconstruction from a standard view [2]. Multi-view reconstruction techniques can combine information from different sets of 2D slices, resulting in a reduction in the reconstruction error. This is useful as for example, in the case of single-view tilt scanning in echocardiography, where the far-field part of the image is sparse, containing much less information than the near-field part. By integrating sweeps from different views, data from the new views can complement the far-field of the first scanning view and improve the reconstruction.

Most ultrasound imaging research on multi-view reconstruction methods focuses on reconstructing the left-ventricle. An example can be found in Ye *et al.,* where a 3D rotational probe and a position sensor are used to track the parasternal short-axis view and apical long-axis view [3]. A rotational probe is used to provide a fixed and regular geometry for the acquired 2D images. Unfortunately, the controller used for providing the fixed geometry tended to be bulky and inconvenient. Legget *et al.* used a 2D freehand scanning protocol to combine long-axis, short-axis, and apical views [4]. However, neither study addressed the problem of how to register 3D reconstructions between different views.

Misregistration is a big problem in freehand 3D ultrasound that affects the accuracy of reconstruction and volume measurement. In general, there are three sources that cause misregistration in freehand 3D ultrasound: (i) error in position and orientation measurements, (ii) target movement during intra-view (non-rigid movement by cardiac motion and respiration) and inter-view scanning (rigid movement of the target), and (iii) probe pressure applied on the scanning surface. Most registration methods reported in the literature use non-rigid registration that describes the movement of the heart using general, elastic spline deformations. Gee *et al.* simplified this general approach by using the mechanics of freehand scanning to define the non-rigid warps used for registration [5]. Shekhar *et al.* described how to use mutual information for both rigid and non-rigid object registration [6]. A landmark volumetric registration by using the first scanning volume as baseline was reported

by Rohling [7]. These registration methods tend to be computationally expensive. Here we'll focus on inter-view registration for multi-view reconstruction.

In this paper, we will only consider position and orientation measurement errors and target motion between views. We will only allow an arbitrary rigid motion of the target between views. We note that the proposed method can be extended to account for all deformations using standard methods for cardiac and respiratory gating. For errors in position and orientation measurements, we present a novel method for estimating the probability density functions (PDF) of the errors and use it to build an interference detector. For rigid-body registration, we use the 3D Hotelling transform to construct a reference volume to quickly register 3D volumes from different views, and in order to overcome the problems with patient movement between sweeps. We also note that our object-based registration method avoids the problem of having to deal with deformation of the scanning surface due to probe pressure between different views sweep. Section 2 describes the proposed methods in detail. Section 3 presents visual and quantitative results in simulated data and phantom data. Concluding remarks and a discussion for future work are given in Section 4.

2. Methods

2.1 Data acquisition

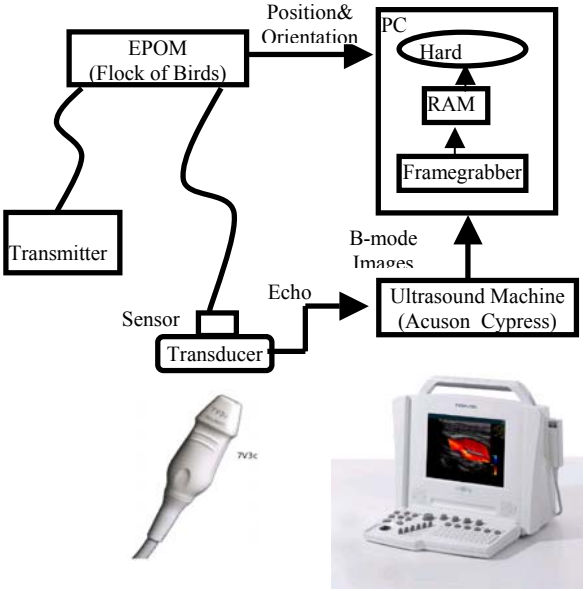

Figure 1. 3D freehand ultrasound imaging system

Figure 1 shows a block diagram of the 3D freehand ultrasound imaging system. The system has been built at the Pediatric Cardiology Clinic of the Children's Hospital Heart Center, at the University of New Mexico. This system has three components: (i) the ultrasound machine, an Acuson Cypress with 7 MHz vector wide-view array transducer (7V3C), (ii) a six-degrees of freedom, electromagnetic position and orientation measurement device (Flock of Birds, Ascension, Burlington, VT, USA), and (iii) a desktop computer (Intel Pentium 4, 2GB memory, 2.6G Hz) equipped with a Meteor-Π Standard framegrabber (Matrox, Canada).

2.2 Electromagnetic interference detector by PDF estimates of EPOM errors

To estimate the probability density function (PDF) of sensor position and orientation error, we move the sensor over three nearly orthogonal planes and collect a large number of points, which are enough to fit the whole plane. The proposed method assumes that there is no bias in the measurements. The algorithm is summarized below:

Step 1. Record a large number of point measurements of the sensor while the sensor is placed over a planar surface.
Step 2. Use least squares to estimate the best fitted plane equation using all point measurements.
Step 3. For each position measurement, compute the positive (above)/negative (below) distance to the best fitting plane.
Step 4. Compute the projections of the sensor's x axis, y axis and z axis onto the normal-vector of the fitting plane.
Step 5. Take the arc-cos of the normalized projections to get the angles and evaluate the deviations from the mean angles .
Step 6. Repeat the above procedures for sensor scanning along three approximately orthogonal planes to estimate the PDF of position x, y, z and orientation angles $x\_angle, y\_angle, z\_angle$

Figure 2. PDF estimates algorithm

We note that the normal vectors of step 4 should be constant because the motion of the sensor on the plane is always a rotation around the normal-vector. We use this fact to estimate the PDFs of the angle error.

Mean square error (MSE) of the position and orientation estimation is used as two-dimensional feature vectors to build a linear classifier for detecting large MSE values due to electromagnetic interference. This classifier is used to automatically detect ferrous interference in the environment. A reward and punishment scheme of the perceptron algorithm [8] is used to build the linear classifier. The N training feature vectors enter the algorithm cyclically, one after the other. If the algorithm has not converged after the presentation of all the samples once, then the procedure keeps repeating until convergence is achieved.

2.3 3D reconstructions from multiple-view sweeping

The 3D system uses a set of arbitrary located 2D image slices in space, as demonstrated in Figure 3. From each image slice, each pixel is transformed to its corrected 3D coordinates in an object-based reference volume. Figure 3 shows the spatial relationships among

the different components: the probe, the 2D ultrasound image, the sensor, and the transmitter.

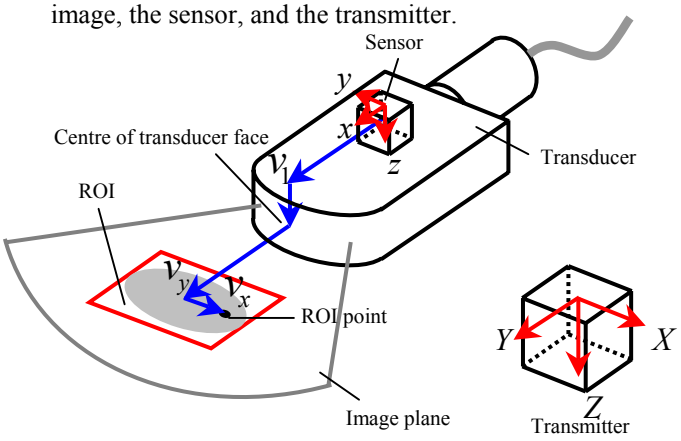

Figure 3. Illustration of spatial relationships in 3D freehand ultrasound

To transform each pixel from each 2D image to its corrected 3D coordinates in the object volume, we apply three coordinate transformations. Firstly, we transform the 2D image coordinates to transducer coordinates, relative to the center of the front face of the transducer. Secondly, we transform the transducer coordinates to 3D sensor coordinates, relative to the origin of sensor coordinate frame. Finally, we transform the sensor coordinates to 3D world coordinates, relative to the origin of transmitter coordinate frame, which is the reconstructed volume.

An averaging strategy is used for combining the multiple views scanning. The intensity of each voxel in the reconstructed volume is estimated by averaging the reconstructed intensities from each view.

2.4 3D registrations by Hotelling transform

The Hotelling transform (also called Principal Component Analysis or Karhunen-Loeve transform) is used for developing our registration method [9]. Assume that the coordinates of each segmented object point are given as random position vectors $\mathbf{X} = [X_1, X_2, X_3]^T$. The mean vector gives the center of gravity of the object given by

$$\mathbf{m}_\mathbf{X} = E\{\mathbf{X}\}.$$

The covariance matrix is given by

$$\mathbf{C}_\mathbf{X} = E\left\{(\mathbf{X}-\mathbf{m}_\mathbf{X})(\mathbf{X}-\mathbf{m}_\mathbf{X})^T\right\}.$$

Each matrix element c_{ii} of $\mathbf{C}_\mathbf{X}$ denotes the variance of x_i, the ith component of the $\mathbf{X}$ vectors. Element c_{ij} is the covariance between components x_i and x_j. For N vector samples from a random population, the mean vector and covariance matrix can be estimated using

$$\mathbf{m}_\mathbf{X} = \frac{1}{N}\sum_{i=1}^{N} x_i,\ \mathbf{C}_\mathbf{X} = \frac{1}{N}\sum_{i=1}^{N} x_i x_i^T - \mathbf{m}_\mathbf{X}\mathbf{m}_\mathbf{X}^T.$$

Given that $\mathbf{C}_\mathbf{X}$ is real and symmetric, it is always possible to find a set of three orthonormal eigenvectors. Define $\mathbf{A}$ to be a matrix whose rows are the eigenvectors of $\mathbf{C}_\mathbf{X}$, ordered so that the first row of $\mathbf{A}$ is the eigenvector that corresponds to the largest eigenvalue of $\mathbf{C}_\mathbf{X}$, and the last row corresponds its smallest eigenvalue. Then

$$\mathbf{Y} = \mathbf{A}(\mathbf{X}-\mathbf{m}_\mathbf{X})$$

is called the Hotelling transform. $\mathbf{C}_\mathbf{y}$ is a diagonal matrix whose diagonal elements are the eigenvalues of $\mathbf{C}_\mathbf{X}$. The components of $\mathbf{Y}$ are uncorrelated.

The new position vectors generated by the Hotelling transform are such that the origin is at the centroid of the object, thus correcting for any object translation, and the transformed object's axes are in the direction of the eigenvectors of $\mathbf{C}_\mathbf{X}$, correcting for arbitrary object rotation. The transformed object's axes are aligned with its principal axes (eigenvectors). The longest axis is positioned in the horizontal direction.

Thus, 3D reconstruction from different views can be registered to the same reference volume.

3. Experimental Results

3.1 PDF estimates of EPOM error and interference detector

For this experiment, we applied the procedure in Figure 2 using 4504 point measurements at a distance between the sensor and the transmitter kept at about 60cm. Figure 4(a) shows the PDF estimates of positional x, y, z measurement errors in an environment that does not have electromagnetic interference. Figure 4(b) shows the orientation angle error x_angle, y_angle and z_angle's PDF estimates.

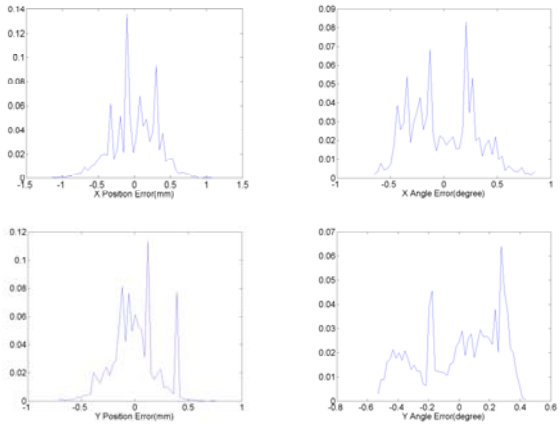

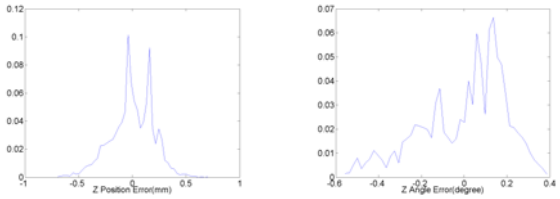

(a) (b)

Figure 4. PDF estimates of sensor measurements. (a) x, y, z position. (b) x_angle , y_angle and z_angle .

The standard deviations for the position errors of x , y , z are 0.2mm, 0.32mm and 0.21mm. The overall root-mean-square (RMS) position uncertainty is estimated to be the Euclidean length of them, which is 0.43mm. This can be easily seen in Figure 4(a), where most of the errors do not exceed a maximum of about ±0.43mm. In Figure 4(b), the standard deviations from the x, y, z mean angles were 0.32°, 0.26°, 0.2° respectively. The overall RMS angle location uncertainty is 0.46°.

Mean square error of the position and orientation estimates is used to define a two-dimensional feature vector for the linear classifier. We collected a data set of 80 feature vectors in different scanning environments. Sixty vectors were used as training set and 20 were left for testing. Perfect separation was achieved during both the training and testing phases, as shown in Figure 5

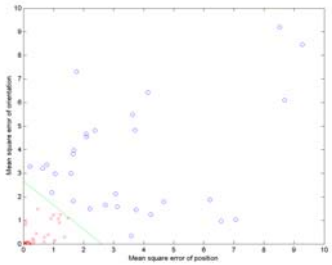

Figure 5. Ferrous interference detection.

3.2 Simulation results for multi-view reconstruction

To compare the reconstruction accuracy for multi-view versus single view reconstructions, we generate a solid ellipsoid with an internal hollow sphere as shown in

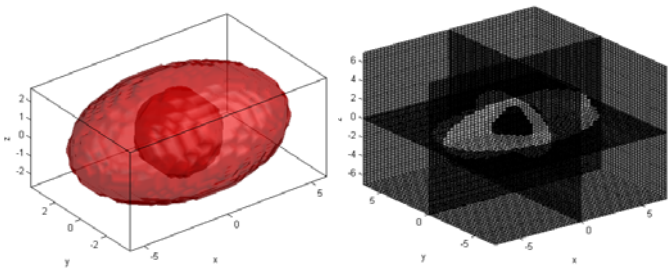

(a)

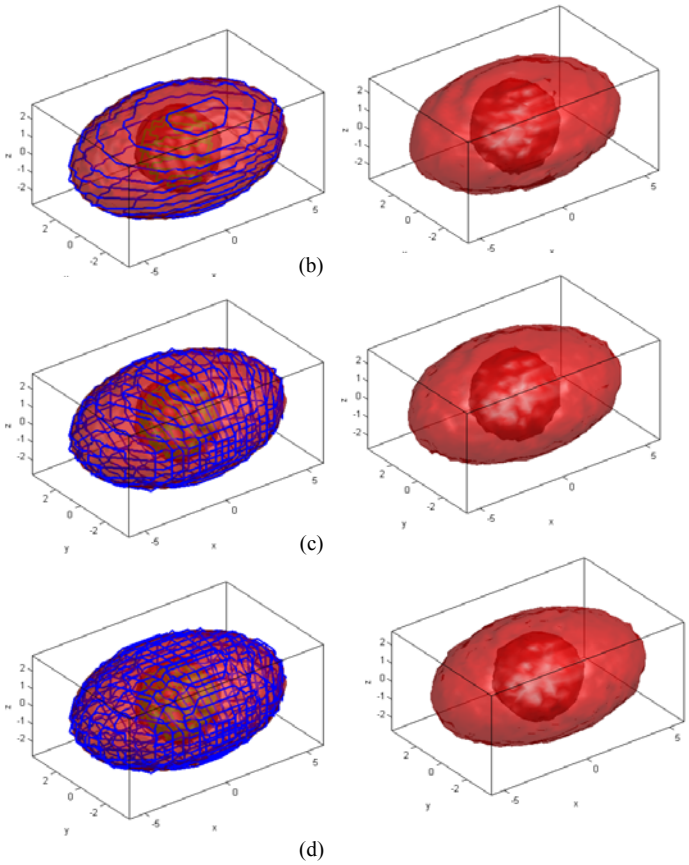

(b) (c) (d)

Figure 6. Simulation results for tilt scanning of test object. (a) original object and three orthogonal plane slices over it, (b) single-view with 30 tilt scanning plane contours in 3D and reconstruction, (c) two-view with 60 tilt scanning plane contours in 3D and reconstruction, (d) three-view reconstruction with 90 tilt scanning plane contours in 3D and reconstruction.

In the experiment, we generated single-view, two-view, and three-view slices, using parallel or tilt scanning planes over the ellipsoid, separately in the x, y, z axis directions, similar to the planes generated during a routine 2D echocardiographic examination [1].

In table 1, we show the mean-absolute-error (MAE) and mean-square-error (MSE) for both parallel and tilt scanning. We clearly see that the reconstruction error is reduced with the increasing number of views. Tilt scanning reconstruction always has a larger error than parallel scanning because tilt scanning results in non-uniform sampling grids in space.

Table 1 Quantitative comparison results of reconstruction (a) mean-absolute-error (b) mean-square-error.

	One-view	*Two-views*	*Three-views*
Parallel	0.0095	0.0059	0.0048
Tilt	0.0178	0.0148	0.0135

(a)

	One-view	*Two-views*	*Three-views*
Parallel	0.0029	0.0014	0.00098
Tilt	0.0057	0.0044	0.0038

(b)

The lack of a 3D registration method can significantly increase the reconstruction error. Even for small displacements. In Figure 7 and Table 2, we show a simple example.

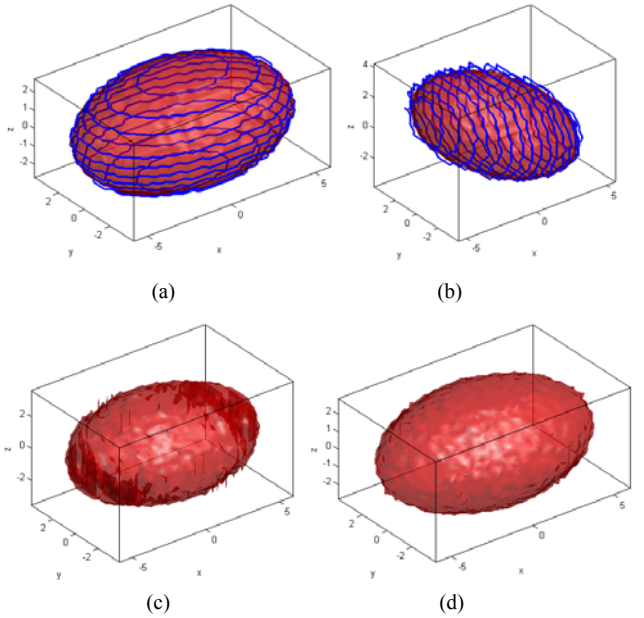

Figure 7 Two-view reconstruction using 3D Hotelling registration. (a) single-view sweep using 30 parallel scanning planes, (b)rotated ellipsoid (rotated around y-axis by 30 degree) is scanned by 30 parallel planes from another view, (c) non-registered two-view reconstruction. (d) registered two-view reconstruction.

A quantitative comparison is provided in Table 2. Both of the MAE and MSE show the registered two-view reconstruction is significantly better than non-registered two-view reconstruction.

Table 2 Quantitative comparison results of Hotelling registration.

Reconstruction Method	*Mean-absolute-error*	*Mean-square-error*
Without 3D volume registration	0.0111	0.0048
With 3D volume registration	0.00638	0.00263

3.3 Validation on real phantom data

The proposed methods were also tested on a 3D ultrasound calibration phantom measured with the freehand 3D ultrasound system described in Section 2.1. These measurements have the disadvantage of being affected by the unsteady probe pressure, spatial locator measurement error, and segmentation error.

Typical B-scans of a small egg target in the phantom are shown in Figures 8(a) and 8(b). In this example, 40 images are used with a region of interest (ROI) 70×70 pixels in the short-axis view and 110×60 pixels in the long-axis view. The manually segmented object contours are shown in Figures 8(c) and 8(d). A smoothed (5×5×5 Gaussian filter (σ = 0.65)) single view reconstruction is shown in Figures 8(e) and 8(f). The long-axis view reconstruction loses some data in the z-axis direction; this is caused by missing data samples and inaccurate segmentation. The reconstructed objects are shown in figures 8(h) and 8(i).

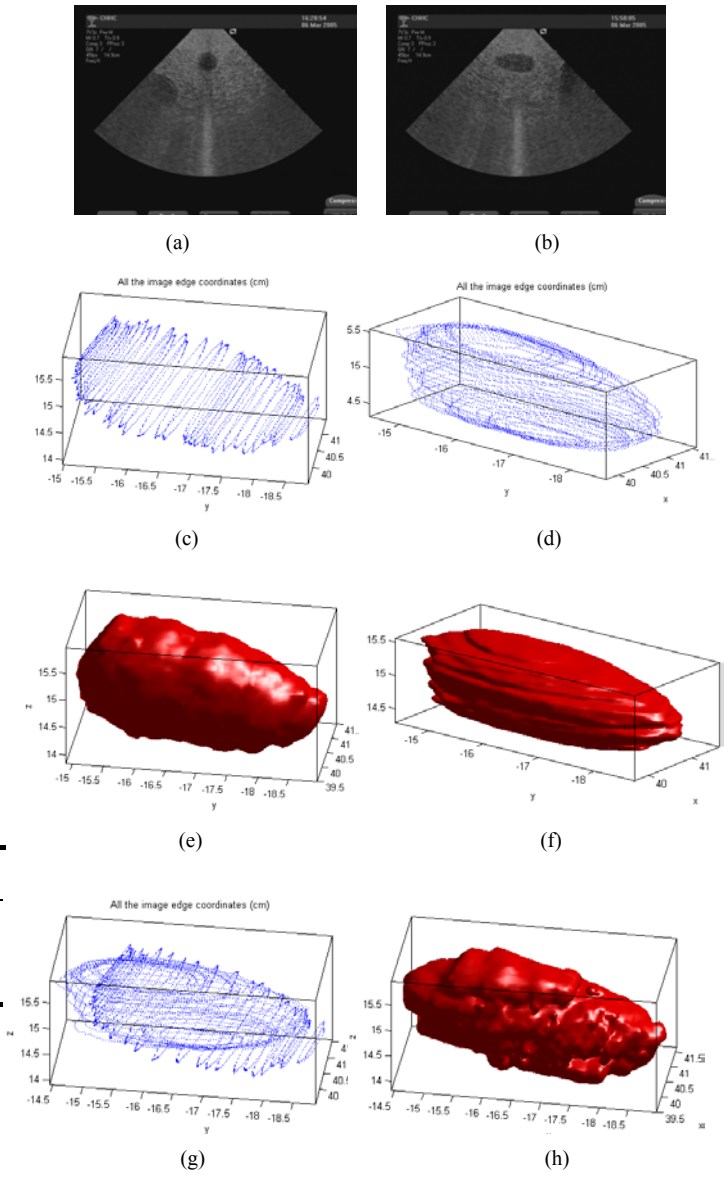

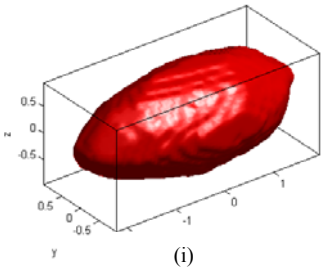

(i)

Figure 8 Multiple-view reconstruction with 3D Hotelling registration. (a) typical short-axis B-scan image (b) long-axis B-scan image. (c) the manual segmented contours in short-axis. (d) manual segmented contours in long-axis. (e) A smoothed short-axis view reconstruction. (f) smoothed long-axis view reconstruction. (g) 3D scanning contours in two views. (h) reconstruction from two-view sweeping. (i) two-view reconstruction by 3D Hotelling registration.

For volume estimation, we used a modified Simpson's rule that is widely-used in echocardiography [1]:

$$V \approx \frac{\pi}{4}\frac{L}{20}\sum_{i=1}^{20} a_i b_i \ .$$

Table 3 shows the volume estimates using 3D volume registration. The two-view reconstruction volume with 3D registration is closer to the real volume (6.9cc) than any single-view reconstruction volume.

Table 3 Volume estimates and relative error (true volume is 6.9cc)

	Short-axis view	*Long-axis view*	*Two-views*
Volume (cc)	7.1357	4.1484	6.8225
Relative error	3.42%	-39.88%	-1.12%

4. Conclusion

A new freehand 3D ultrasound imaging system has been developed. The proposed multi-view reconstruction system has been shown to give more accurate 3D reconstructions for both simulated data and phantom data compared to a single view or multi-view non-registered reconstruction. In order to achieve robust performance, a new interference detection system is used, which can be used to estimate the probability density function for both position and angle measurements of the acquired 2D slices. Robust reconstruction is achieved through the use of an object-based, 3D volume registration system, which is shown to increase the accuracy of reconstruction with the number of distinct views used. For reconstructing deformable objects, the proposed methods can be extended to use cardiac and respiratory gating to guarantee that only rigid object motions occur between gated 3D slices.

Our current research is focused on analyzing the performance of the system for (i) both additive and multiplicative noise, (ii) a variety of different, automated segmentation systems, and (iii) allowing for realistic deformation within intra-view acquisition. In particular, we are interested in quantifying the amounts of noise, segmentation error, and intra-view motion that can be tolerated, while still allowing us to produce acceptable 3D reconstruction and volume measurements

References

[1] A.R.Snider, G.A.Serwer, S.B.Ritter, and R.A.Gersony, Echocardiography in pediatric heartdisease, 2nd ed, St. Louis : Mosby, 1997

[2] A.Fenster, D.B.Downey, and H.N.Cardinal, "Three-dimensional ultrasound imaging," Physics in medicine & biology, vol. 46, pp. R67-99, 2001

[3] X.Ye, J.A.Noble and D.Atkinson, "3-D freehand echocardiography for automatic left ventricle reconstruction and analysis based on multiple acoustic windows", *IEEE transaction on medical imaging*, vol.21, pp. 1051-1058, 2002.

[4] M.E.Legget, D.F.Leotta, E.L.Bolson, J.A.McDonald, R.W.Martin, X.N.Li, C.M.Otto, and F.H.Sheehan,"System for quantitative three- dimensional echocardiography of the left ventricle based on a magnetic-field position and orientation sensing system," *IEEE transactions on biomedical engineering*, Vol.45, pp.494-504, 1998.

[5] A.H.Gee, G.M.Treece R.W.Prager, C.J.C.Cash, and L.Berman, "Rapid registration for wide field of view freehand three-dimensional ultrasound", *IEEE transactions on medical imaging*, Vol.22, pp. 1344-1357, 2003.

[6] R.Shekhar, and V.Zagrodsky, "Mutual information-based rigid and nonrigid registration of ultrasound volumes", *IEEE transactions on medical imaging*, vol.21, pp. 9- 21, 2002

[7] R.N.Rohling, A.H.Gee, and L.Berman, "Automatic registration of 3-D ultrasound images", Ultrasound in medicine & biology, Vol.24, pp.841-854, 1998

[8] S.Theodoridis and K.Koutroumbas, *Pattern Recognition*: Academic Press, 1999

[9] R.C.Gonzalez, and R.E.Woods, *Digital image processing,* Prentice Hall, 2002